Unraveling the auxin mechanism in 2,4-D induced somatic embryogenesis in Arabidopsis thaliana

Philipsen, C.

Chapter 2

2,4-D-induced somatic embryogenesis initiation requires a relative auxin minimum in *Arabidopsis*.

Cheryl Philipsen[1,2],
Remko Offringa[1]

[1.] *Molecular and Developmental Genetics, Institute of Biology Leiden, Universiteit Leiden, Sylviusweg 72, 2333BE, Leiden, Nederland*
[2] *Current affiliation: Dümmen Orange, P.O. Box 26, 2678ZG, de Lier, the Netherlands*

Abstract

Techniques for clonal plant propagation are important to high economically valued crops and ornamentals and it comes in many forms, including the process of somatic embryogenesis (SE). In *Arabidopsis*, SE can be efficiently induced by treatment of immature zygotic embryos (IZEs) with the synthetic auxin analog 2,4-dichlorophenoxyacetic acid (2,4-D). The natural auxin indole-3-acetic acid (IAA) and its cellular transport play an important role in zygotic embryogenesis (ZE) as well as organogenesis; however, the involvement of IAA in 2,4-D induced SE initiation is yet unclear. To investigate this we established a standardized system for SE initiation and outgrowth of somatic embryos using 12 days old *Arabidopsis* IZEs. In this system, *pWOX2::NLS-YFP* was used as a marker for embryonic cell fate and the first *WOX2-YFP*-reported embryonic cell clusters could be observed after 5 to 7 days of culture in somatic embryogenesis inducing medium (SEIM). Interestingly, these clusters were located in regions of low auxin response. Studies using inhibitors of cellular auxin transport indicated an important role for auxin influx in SE initiation, whereas auxin efflux only seemed to be important for establishment of the embryonic body pattern later during SE. In fact, *aux1 lax* loss-of-function mutant IZEs showed enhanced shoot/root regeneration at the cost of SE. Expression of AUX1 influx carriers directly next to the SE initiation sites suggested that auxin influx might be necessary for generating the low auxin response regions that are important for SE initiation.

Introduction

Clonal plant propagation can be achieved by simple stem-, leaf- or root cuttings, or by more elaborate tissue culture-based methods where shoots and subsequently roots, or even complete embryos are regenerated from plant tissues. In the latter process, referred to as somatic embryogenesis (SE), somatic plant cells derived from late embryogenic or vegetative tissues develop into embryos. In contrast to zygotic embryogenesis (ZE), SE does not require fertilization as an initial trigger, but it still results in an embryo with a complete root-shoot axis, vascular system and functional meristems (Pupilli and Barcaccia, 2012; Fehér, 2015). SE is desirable as a strategy for stable clonal propagation, of for example F1 hybrid crops, since the resulting embryos can be cryopreserved for later use or to establish gene banks (Timmis, 1998; Arnold et al., 2002) and it allows the production of unlimited numbers of normal individuals using bioreactors (Timmis, 1998). Moreover, as opposed to shoot/root regeneration, SE has been reported to result in limited somaclonal variation among the propagated individuals, (reviewed by Gaj, 2004; Bairu et al., 2011). SE is also used as an alternative method to study ZE in species that have a long reproduction cycle and with economic relevance, such as spruce (*Pinacea*) (Timmis, 1998; FAO, 2015). SE provides the advantage of producing a high number of individual somatic embryos and thus the process of embryogenesis can be studied on a large scale within a shorter time frame. One has to keep in mind, however, that SE and ZE are different processes that are initiated by different signals.

Several genes have been identified as key regulators of SE. These include *LEAFY COTYLEDON1 (LEC1)* and *LEC2, FUSCA3 (FUS3), BABY BOOM (BBM)* and *WUSCHEL (WUS)* (Lotan et al., 1998; Stone et al., 2001; Boutilier et al., 2002; Zuo et al., 2002). *LEC1, ABA INSENSITIVE3* (*ABI3*), *FUS3, and LEC2* constitute the *LAFL* gene network, that was initially identified based on its role in seed maturation and the transition from embryo to seedling development (Jia et al., 2013). Later, it was shown that *lec1*, *lec2* and *fus3* loss-of-function mutants are impaired in their competence to form somatic embryos (Gaj et al., 2005), whereas constitutive overexpression of *LEC1* and *LEC2* leads to spontaneous SE on the shoot apical meristem and cotyledons of germinating seedlings (Lotan et al., 1998; Stone et al., 2001). Overexpression of *FUS3* leads to development of cotyledon-like leaves by holding these post embryonic tissues in a phase that benefits the embryogenic capacity (Gazzarrini et al., 2004). The action of the *LAFL* genes seems to depend on levels of the seed maturation hormone abscisic acid (ABA). ABA is required for *LEC1*- and *LEC2*-induced embryonic differentiation, which subsequently activates

endogenous auxin production and results in reprogramming of epidermal cells generating callus and somatic embryos (Stone et al., 2008; Junker et al., 2012).

The induction of SE in different plant species often requires treatment of somatic tissues with 2,4-dichlorophenoxyacetic acid (2,4-D), a synthetic analog of the plant hormone auxin, indole-3-acetic-acid (IAA). The natural IAA generally cannot induce this process, which is surprising in view of the important role of this signalling molecule during early zygotic embryogenesis (Friml et al., 2003; Rademacher et al., 2012), and the importance of an elevated auxin response downstream of the *LAFL* gene network and ABA in inducing SE (Michalczuk et al., 1992; Pasternak, 2002; Gaj et al., 2005; Su et al., 2015). In zygotic embryogenesis the auxin responses patterning the embryo are governed by differential distribution of auxin by polar cel-to-cell transport of auxin (Weijers et al., 2005; Robert et al., 2013, 2015b). Here, we investigated the role of auxin transporters in regulating auxin responses during 2,4-D induced SE initiation from *Arabidopsis* immature zygotic embryos (IZEs).

Polar auxin transport (PAT) involves the activity of three families of membrane proteins (Petrásek and Friml, 2009; Swarup and Péret, 2012). In line with the chemiosmotic hypothesis that was initially proposed to provide a mechanistic basis for the cell-to-cell auxin flow (Rubery and Sheldrake, 1974; Raven, 1975; Goldsmith, 1977), auxin can diffuse over the plasma membrane in its protonated form, but its uptake is also facilitated by AUX1/LIKE AUX1 (AUX1/LAX) influx carriers that form a small family of four proteins in *Arabidopsis* (AUX1, LAX1, LAX2 and LAX3). AUX/LAX proteins are thought to enhance the steady-state concentration of auxin in plant cells, and were found to be important drivers of PAT (Swarup et al., 2005; Jones et al., 2009; Boot et al., 2015). AUX1 and LAX3 function in gravitropism (Swarup et al., 2001) and lateral root development (Marchant et al., 2002; De Smet et al., 2007; Swarup et al., 2008), LAX2 regulates vascular patterning in cotyledons (Peret et al., 2012) and AUX1, LAX1 and LAX2 are required in different stages in zygotic embryo development (Ugartechea-Chirino et al., 2010; Peret et al., 2012; Robert et al., 2015b). The role of AUX/LAX in SE is not well established yet.

The chemiosmotic hypothesis for PAT predicts that due to the basic pH inside plant cells auxin is mostly deprotonated, and that as a negatively charged ion, auxin can only pass the plasmamembrane (PM) with the help of efflux carriers. Asymmetric distribution of these efflux carriers on the PM of the cell generates a polar cell-to-cell flow of auxin. Research in *Arabidopsis* has identified two types of auxin efflux carrier. First, the PIN-FORMED (PIN) proteins that have been shown to be the rate limiting components that direct PAT through their asymmetric distribution at the PM of the cell (Petrásek et al., 2006; Wisniewska, 2006). Secondly,

the ABCB/MULTIDRUG RESISTANCE/P-GLYCOPROTEIN class of transporters that do not exhibit polarity and have been proposed to determine the amount of auxin available for PIN-mediated PAT (Geisler and Murphy, 2006; Mravec et al., 2008). In *Arabidopsis thaliana*, PIN proteins are encoded by a small gene family of eight members. The protein structure of PINs is highly conserved and consists of two transmembrane domain regions separated by a hydrophilic loop that varies in length (Friml et al., 2002; Benková et al., 2003; Friml et al., 2003; Blilou et al., 2005; Mravec et al., 2009). PINs with a long hydrophilic loop (long PINs) are localized on the PM (PIN1, 2, 3, 4 and 7) whereas PINs with a short hydrophilic loop (short PINs) are localised in the endoplasmatic reticulum (ER) (PIN5 and PIN8). PIN6 contains a hydrophilic loop of intermediate length and is localised both in the ER and at the PM (Mravec et al., 2009; Sawchuk et al., 2013; Ganguly et al., 2014). Asymmetric localisation by PINs results in local dynamic auxin maxima and minima or gradients that are instructive in many developmental processes, including embryo patterning (Friml et al., 2003; Robert et al., 2015b), tropic growth (Luschnig et al., 1998; Friml et al., 2002) and organ formation (Reinhardt et al., 2000; Benková et al., 2003). All the long PINs have been shown to be involved in patterning the zygotic embryo by generating auxin maxima that first mark the early embryo proper, then organise the root pole, and finally position the cotyledon primordia (Friml et al., 2003; Blilou et al., 2005). During SE PIN1 is proposed to act by mediating auxin transport from areas with high auxin towards areas of low auxin prior to establishment of the somatic embryo (Su et al., 2009), and PIN4 was shown to be uniformly expressed in cell clusters and restricted to the embryonic root as development progresses (Bassuner et al., 2006). These findings suggest a developmental role for PINs during SE.

In order to test the involvement of PAT in SE, we first optimized the *Arabidopsis* system for 2,4-D-induced SE from IZEs for our culture conditions. By making use of the embryonic cell fate reporter *pWOX2::NLS-YFP* (Breuninger et al., 2008; Haecker et al., 2004) and combining this with the well-known *DR5* auxin response reporter (Ulmasov et al., 1997), we could show that SE is initiated in IZEs between 5 and 7 days after the start of 2,4-D treatment in areas of low *DR5* response. This is in contrast to the auxin maxima that mark the positions of lateral organ initiation in the shoot meristem and in the root (Reinhardt et al., 2003; Benková et al., 2003) (Reinhard 2003, Benkova 2003). Inhibitor studies indicated that auxin influx rather than efflux is crucial for SE initiation. The expression of the AUX1 influx carrier in cells next to the SE initiation sites suggested that auxin influx is required to generate the relative auxin response minimum that allows SE initiation.

Results

A standardized procedure for SE induction and scoring on Arabidopsis IZEs

Even though several protocols have been published on 2,4-D induced SE on *Arabidopsis* IZEs (Gaj et al., 2005; Su et al., 2009; Nowak et al., 2012), we experienced quite some variation in the efficiency of SE per experiment. Since comparing different treatments and *Arabidopsis* mutants for SE efficiency required a robust and reproducible protocol, we decided to optimize the protocol for our laboratory conditions. Thus far, most protocol optimizations have focused on medium composition. Here we mainly considered the workflow (Figure 1) of the SE protocol, with a focus on the culture time and the developmental stage and the physiology of the IZEs, (Luo and Koop, 1997; Gaj, 2001; Jiménez, 2005). Most protocols use 'late' IZEs, where the two cotyledons are folded beside the hypocotyl-root. Since the 'folded' phenotype is rather a subjective criterion, we aimed at culturing IZEs for which the development was synchronized by harvesting them at 9, 11, 12, 14 and 15 days after pollination (dap), on solid somatic embryogenesis inducing medium (SEIM) for 14 days, and on hormone free medium for 7 days. Experiments were either scored for SE efficiency, which is the number of IZE explants producing somatic embryos and embryonic structures, or for SE productivity, where we determined the average number of somatic embryos formed per IZE. The SE efficiency appeared to be a stable parameter that allowed to assess SE between experiments, whereas SE productivity varied strongly between experiments (0.2 – 3.8 somatic embryos/IZE, Figure S1) and was more dependent on the observer and it is therefore important to always include an untreated or wild-type control into the experiment. To improve uniformity in SE productivity scoring, we defined more clearly the structures that developed during culturing and were taken along in the score. For SE productivity, only individual somatic embryos were counted that showed a smooth green surface, developed their own vascular system (Bassuner et al., 2006), and were only connected to the IZE explant at the root tip (Figure 2a,b).

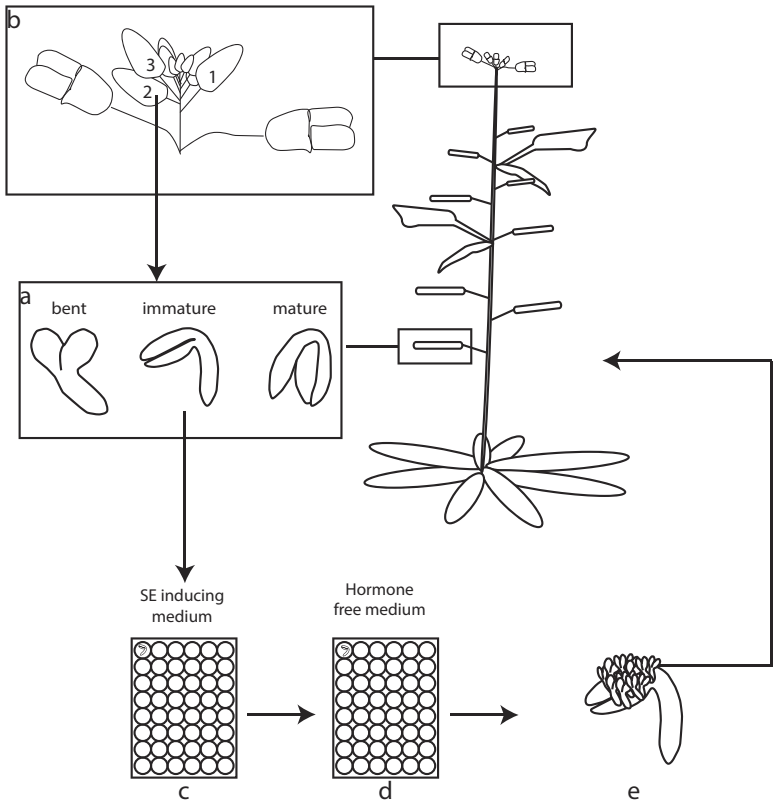

FIGURE 1 - Workflow of somatic embryogenesis (SE) on *Arabidopsis thaliana* immature zygotic embryos (IZEs).
IZEs were either harvested from siliques and size-selected (a), or the three most mature closed flower buds were emasculated and pollinated and IZEs were harvested at specific days after pollination (b). SE was induced by culturing the IZEs on SEIM for 14 days (c), after which they were transferred to hormone free medium for 7 days to allow outgrowth of the somatic embryos to facilitate scoring (d). Somatic embryos germinated and grew out to a full mature plant when detached from the explant and germinated on hormone free medium (e).

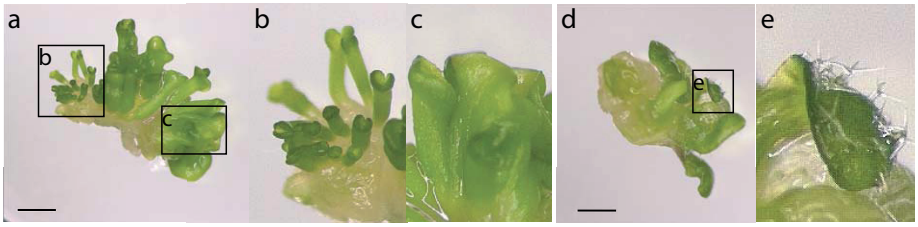

FIGURE 2 - Overview of the different tissues developing from *Arabidopsis* IZEs.
a) and d) two *Arabidopsis* (Col-0) IZEs after standard SE culture (see M&M). b) and c) are enlargements of the indicated regions in a), showing either individual somatic embryos with an individual root pole (b) or fused embryonic structures (c). e) Detail of the region in c) showing a shoot-like structure with a rough green surface and trichomes. Scale bar represents 1mm.

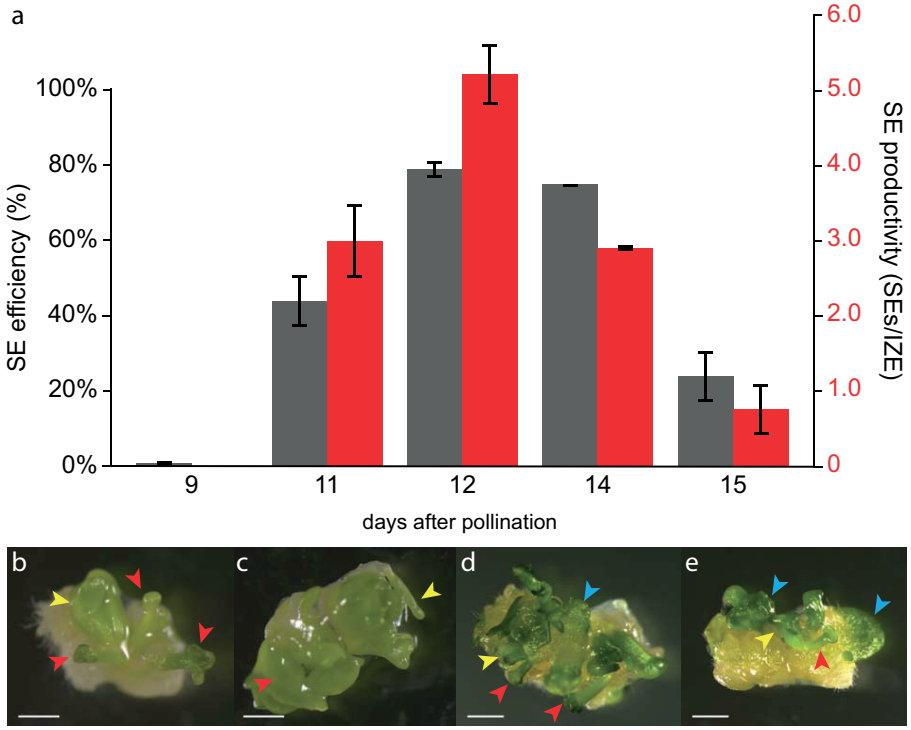

FIGURE 3 - SE efficiency and productivity strongly depend on the age of the *Arabidopsis* IZEs.
a) SE efficiency (grey bars) and SE productivity (red bars) of *Arabidopsis* IZEs after standard SE culture. SE efficiency is expressed as the number of IZEs producing embryonic callus and somatic embryos and SE productivity is expressed as number of individual somatic embryos produced per IZE. Bars represent average of duplicate experiments, with n=48. Error bars indicate the standard error of the mean (SEM). $\chi 2$ test for association showed that the SE efficiency is significantly determined by the age of the IZE ($\chi 2$=85.6, p<0.05). b-e) *Arabidopsis* IZEs harvested at 11 (b), 12 (c), 14 (d), or 15 dap (e) after standard SE culture. Red arrowheads indicate individual somatic embryos, yellow arrowheads indicate embryonic structures, and blue arrow heads point out shoot-like structures. Scale bar represents 1mm.

Somatic embryos fused along the hypocotyl-cotyledon axis into embryonic structures were too difficult to accurately count and were therefore only taken along for the SE efficiency (Figure 2a,c). By scoring this way, we took into account that the SE productivity provided an underestimate of the total number of somatic embryos per explant. Obviously, shoot-like structures that exhibited a rougher darker green surface and trichomes (Figure 2d,e) were not scored as somatic embryos. Using these criteria, we observed the highest SE efficiency with IZEs that were harvested 12 or 14 dap, and the highest SE productivity in 12 dap IZEs (Figure 3a). Although some 11 dap IZEs were capable of producing individual somatic embryos (Figure 3b,c), most of the IZEs died during culturing on SEIM in the first 7 days, resulting in a low SE efficiency. IZEs of 9 dap mostly died during culture, and most 15 dap IZEs produced shoot-like structures rather than somatic embryos (Figure 3e). A χ^2 test for association showed that the SE efficiency depends on the IZE age ($p<0.05$). Since both SE productivity and SE efficiency were high at 12 dap, this time point was selected for IZE harvesting.

SE initiation in IZEs requires 5 days 2,4-D induction

With the SE protocol optimized using 12 dap IZEs, our next aim was to use a reporter to identify embryonic cells during SE initiation. Several embryonic cell reporters have been described previously (Haecker et al., 2004; Soriano et al., 2013), but some of these reporters marked the suspensor rather than the embryo proper during zygotic embryogenesis. In contrast, the *pWOX2::NLS-YFP* reporter specifically marked the zygotic embryos from early stages on (Haecker et al., 2004; Breuninger et al., 2008, Figure S2), and seemed ideal for the purpose of tracing the initiation and early phases of SE. Time lapse imaging of IZEs by confocal microscopy every 24 hours starting from day 8 in culture showed that *pWOX2::NLS-YFP* expressing cells could already be observed at day 8 (Figure 4a), and over days 10 to 14 these cells grew out to *pWOX2::NLS-YFP* expressing protuberances that resembled globular shaped zygotic embryos (Figure 4b-d). *pWOX2::NLS-YFP* expressing cells were observed on both adaxial and abaxial sides of the cotyledons, mostly located at the base of the cotyledons (the proximal area). The *pWOX2::NLS-YFP* expressing protuberances developed on top of callus tissue that did not express *pWOX2::NLS-YFP* or only at a low level (Figure 4d). Based on this observation, the fact that the *WOX2-YFP* reporter marks the early zygotic embryo (Breuninger et al., 2008), and that the expressing protuberances grew out to somatic embryos when followed in time we concluded that *pWOX2::NLS-YFP* is a suitable marker to track SE from initiation to development of the somatic embryo and thereby as a marker for cells that revert their cell fate from 'late' embryogenic to 'early' embryogenic.

Next, we looked at earlier time points to more accurately determine the minimum 2,4-D exposure time required of SE initiation by incubating *pWOX2::NLS-YFP* IZEs for 3, 5 or 7 days on SEIM, and subsequently for 48hr to hormone free medium (Figure 4e-i). Incubation on SEIM for 5 and 7 days, but not 3 days, resulted in *pWOX2::NLS-YFP* expressing cells in the proximal region of the cotyledons (Figure 4e,f,g). However, these positive cells did not develop into strong foci of YFP expression, but instead YFP positive cells remained more dispersed in the proximal region of the cotyledons compared to their controls (Figure 4h,i). This suggested that the patterning programme of the somatic embryo is abolished after transfer to hormone free medium. A phenotypic study of IZEs that were grown for 3, 5 or 7 days on SEIM and subsequently transferred to hormone free medium to allow somatic embryos to develop for a subsequent 7 days (Figure 4j-m) showed that IZEs grown for 3 days on SEIM continued to germinate after transfer to hormone free medium and developed into seedlings with aberrations (Figure 4l). IZEs incubated for 5 days on SEIM showed mostly seedling growth, but on average 53% developed embryonic structures (Figure 4k). The 7 days SEIM incubation resulted in a similar SE efficiency (76%) as the standard 14 days protocol, whereas the SE productivity lagged behind considerably (Figure 4j). A χ^2 test for association showed that the SE efficiency was significantly dependent on the duration of 2,4-D treatment ($p < 0.05$). These results indicated that 5 days 2,4-D exposure was sufficient for IZE cells to be reprogrammed and revert their cell fate, but also that a longer 2,4-D exposure is required to establish multiple stable foci of *WOX2* expression that give rise to a reasonable number of individual somatic embryos.

2,4-D induced somatic embryos occur in areas of relatively low auxin response

To investigate the correlation between early somatic embryo initiation and auxin response we combined the *pWOX2::NLS-YFP* embryo marker with the *DR5::RFP* auxin response reporter. At 3 and 4 days after 2,4-D treatment, the auxin response was relatively low throughout the entire IZE (Figure 5a,b). At day 5, however, the auxin response increased both in the cotyledons (Figure 5c) and the hypocotyl (Figure 5e,f,i). *pWOX2::NLS-YFP* expression was again first observed at day 5, mostly in cells in the proximal region on both adaxial and abaxial sides of the cotyledons and in a few cells in the hypocotyl (Figure 5c-f). Simultaneously, we observed that the auxin response was overall increasing, but that local auxin response minima developed on day 5, coinciding with cells expressing *pWOX2::NLS-YFP* (Figure 5d-f). Remarkably, this is in contrast to lateral organogenesis in the shoot apical meristem (SAM) or root, where auxin maxima mark the onset of organ initiation (Benková et al., 2003; Friml et al., 2003; Heisler et al., 2005; Marhavý et al., 2013). These findings suggest that the auxin response

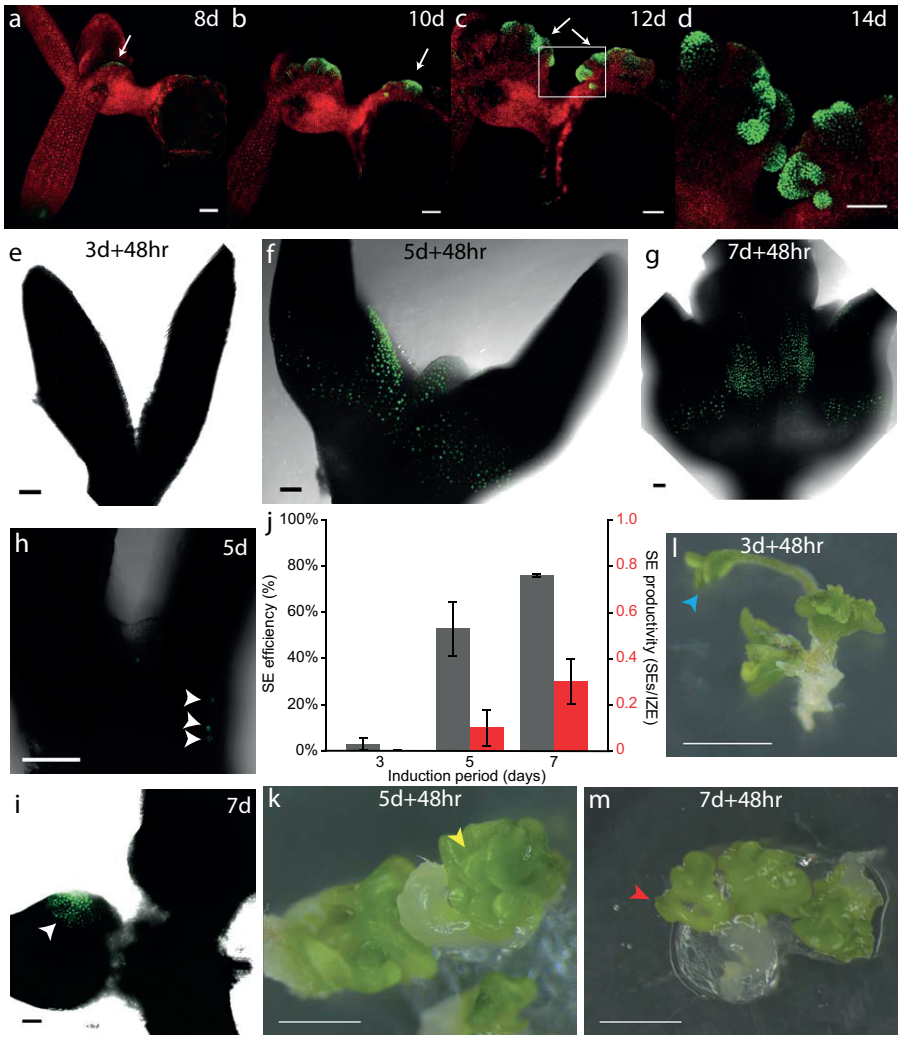

FIGURE 4 - SE in *Arabidopsis* IZEs is initiated between 5 and 7 days of culture.
a - d) Timelapse of *pWOX2::NLS-YFP* (green) expression in *Arabidopsis* IZEs after 8 (a), 10 (b), 12 (c) or 14 (d) days of culture on SEIM. Chlorophyl in red, arrows point to cells expressing *pWOX2::NLS-YFP*, scale bar represents 100µm. e-i) *pWOX2::NLS-YFP* (green) expression in IZEs after 3 days SEIM + 48hr hormone free (e) 5 days SEIM + 48hr hormone free (f) 7 days SEIM + 48hrs hormone free (g), controls of 5 days SEIM in (h) and 7 days SEIM in (i), white arrow heads point at cells expressing *pWOX2::NLS-YFP*. j - m) phenotype study of hormone free treatment with j) SE efficiency (grey bars) and productivity (red bars) for each initiation period. Bars represent average of duplicate experiments, with n=48. Error bars are SEM, $\chi 2$ test for association was used, $\chi 2=70.7$, $p=0.05$. l-m) Phenotypes of IZEs with SEIM induction for l) 3 days k) 5 days m) 7 days. Red arrowhead point at individual somatic embryos, yellow arrowhead point at embryonic like structures and blue arrowhead are dedicated to shoot like structures. Scale bar is 1mm.

is regulated in a spatiotemporal manner during SE initiation. To investigate whether this dynamic auxin response was required for SE initiation, we stopped SE induction after three days by transferring IZEs to hormone free medium and incubating them for 48 hours. We noticed that the auxin response was lost, both in cotyledons (Figure 5g vs 5h) and in the hypocotyl (Figure 5i vs 5j). Simultaneously, *pWOX2::NLS-YFP* was also absent in the cotyledons, confirming that SE initiation was inhibited. Interestingly, during incubation on hormone free medium, an increase in *pWOX2::NLS-YFP* expression could be observed in the hypocotyl, indicating that the cells in the hypocotyl maintained their embryonic identity, and suggesting that 2,4-D is required to downregulate this *WOX2* expression in the hypocotyl and to reprogram cells in the cotyledons to induce SE.

Auxin response minima coinciding with SE initiation require auxin influx proteins

The auxin dynamics in the cell reported by the *DR5::RFP* marker is the sum of auxin homeostasis (biosynthesis, conjugation and turn over), transport and signalling. All three pathways have been reported to be important for zygotic embryogenesis (Hardtke and Berleth, 1998; Friml et al., 2003; Cheng, 2006; Weijers et al., 2006; Rademacher et al., 2012; Robert et al., 2013, 2015b). To study auxin transport, we used the inhibitors N-1-napthylphthalamic acid (NPA) (Noh et al., 2001) or 1-naphthoxyacetic acid (1-NOA) (Parry et al., 2001) to chemically block respectively auxin efflux- or auxin influx activity from the start (0d), before establishment of the first embryonic cells (3d) or during establishment of the first embryonic cells (5d). As controls, we included IZEs continuously grown on SEIM (0d ctrl) or IZEs that were transferred to fresh SEIM plates after 5 days of culture on SEIM (5d ctrl). Blocking active auxin efflux with 100µM NPA did not affect SE initiation as severely as was expected based on genetic data on zygotic embryogenesis (Figure 6a) (Friml et al., 2003; Blilou et al., 2005). NPA treated IZEs developed both individual somatic embryos as well as embryonic structures (Figure 6g-i). However, the derived somatic embryos appeared to be smaller and more often fused compared to the control. Only NPA treatment of IZEs from the start of their incubation on SEIM resulted in a significant reduction in SE efficiency (60%), but the SE productivity, i.e. the development of the individual somatic embryos, was significantly reduced for day 0 (0.7 somatic embryos/IZE) and day 3 (0.7 somatic embryos/IZE) compared to the control (1.3-1.5 somatic embryos/IZE). Examination of the *WOX2 DR5* reporters showed no obvious perturbation in the spatiotemporal distribution of the auxin response in NPA treated IZEs. NPA treatment still allowed SE initiation to occur in local relative auxin minima (Figure 6f), similar to the control (Figure 6b). In conclusion, auxin efflux is not responsible for generating such local auxin response minima.

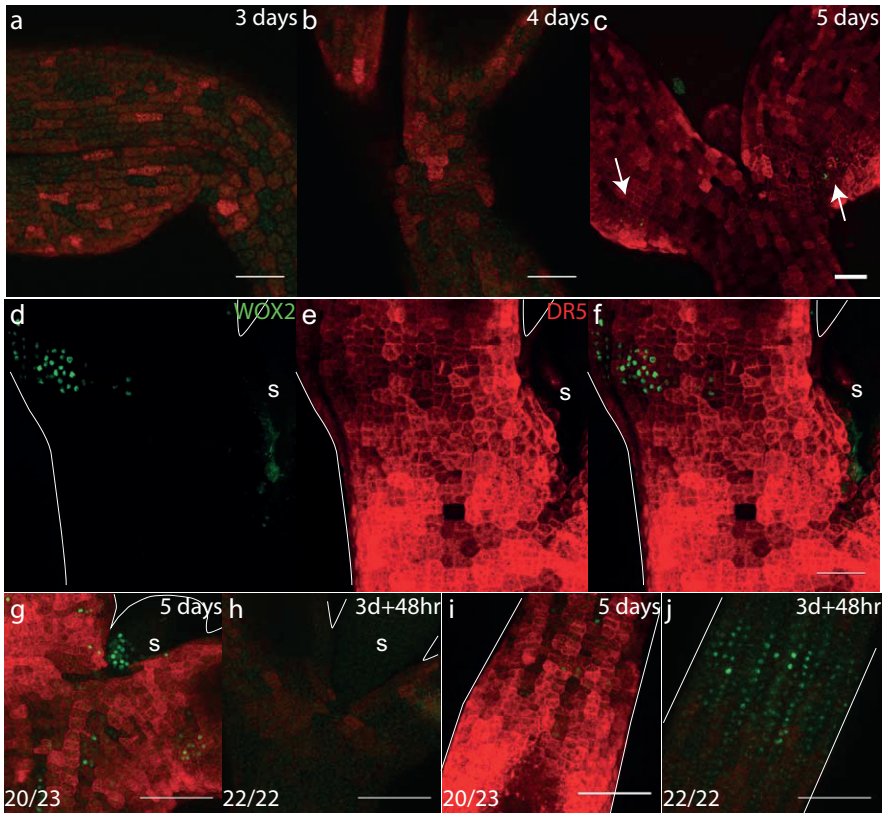

FIGURE 5 - Dynamic auxin responses during SE initiation in *Arabidopsis* IZEs.
Representative CLSM images of *pWOX2::NLS-YFP* (green) *DR5::RFP* (red) IZEs, cultured on SEIM for 3 days (a,g,h,j), 4 days (b) and 5 days (c,d-f,i). Images in (a-c, f, g-j) show both the YFP and RFP signal, whereas (d) and (e) represent respectively the separate YFP and RFP signals in (f). g,i) An IZE with 5 days SEIM induction vs h,j) is an IZE with 3 days induction + 48 hr hormone free treatment. Observation frequencies are indicated in the left bottom, scale bar is 50um (a-c) or 100µm (g-j).

In contrast, treatment with the auxin influx inhibitor NOA resulted in a significant reduction of the SE efficiency and -productivity for all three time points (Figure 6a). The NOA-treated IZEs mostly developed small whitish calli with dark green leaf-like structures or an occasional embryo-like structure (Figure 6k-m). These findings are supported by the *WOX2-YFP* expression, showing that no embryonic cell fate was initiated (Figure 6j). The auxin response was still strong upon treatment with 1-NOA, but in contrast to the control, this response seemed more evenly distributed without the generation of local auxin minima. Our observations suggest that auxin influx is necessary for embryonic cell fate initiation by creating local auxin minima, and that auxin efflux rather plays a role in the further development of these cells into somatic embryos.

A recent publication has indicated the involvement of auxin influx in zygotic embryogenesis, where the AUX1, LAX1 and LAX2 influx carriers are the main contributors that supply the PAT system with auxin (Robert et al., 2015b). To investigate which influx carriers are required and to confirm our findings with 1-NOA we

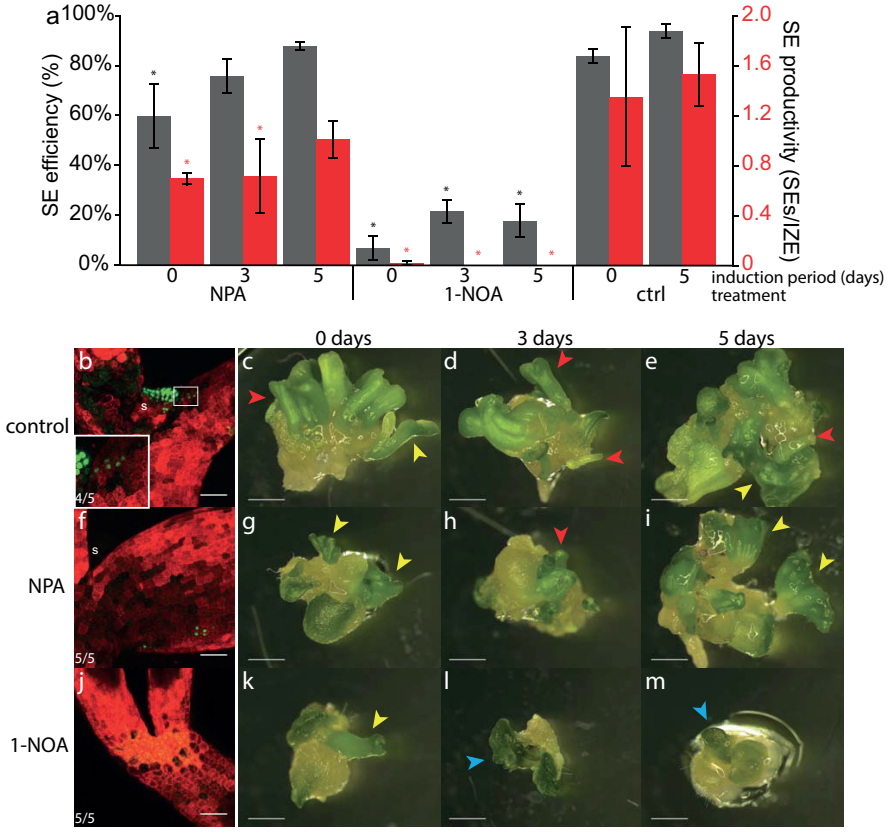

FIGURE 6 - Auxin influx rather than -efflux is essential for SE initiation in *Arabidopsis* IZEs.

a) SE efficiency (grey bars) and productivity (red bars) of IZEs incubated on SEIM to which 100uM NPA or 1-NOA was added at the start or at 3 or 5 days after the start of the incubation. Control IZEs were incubated on SEIM without (0) or with transfer to fresh SEIM after 5 days (5). Bars represent values of duplo experiments with n = 48, error bars indicate SEM. Asterisks denote statistical difference between control and treatment. SE efficiencies were compared using the $\chi 2$ test ($p<0.05$), and SE productivities were compared using the Welch *t*-test ($p<0.05$). b, e, h) Representative CLSM images of *pWOX2::NLS-YFP* (green) *DR5::RFP* (red) IZEs cultured for 3 days on SEIM followed by 48hr on hormone free medium, in the absence (b) or presence of 100µM NPA (f) or 100µM 1-NOA (j). Scale bar represents 50µm. Numbers represent observation frequencies (c-e). Phenotype of control treatment (2,4-D) with (c) 0 days (d) 3 days (e) 5 days. Phenotype of NPA with (g) 0 days (h) 3 days (i) 5 days. (k - m) phenotype of 1-NOA with (k) 0 days (l) 3 days (m) 5 days. Red arrow heads point at individual somatic embryos, yellow arrow heads pointed at embryogenic structures and blue arrow heads indicate shoot-like structures, observation frequencies are indicated the bottom right corner, scale bar represents 1mm.

determined the SE efficiency of the *Arabidopsis aux1 lax1*, *aux1 lax2* and *aux1 lax3* double mutants and compared this to wild type (Figure 7). In these experiments we noticed that many of the mutant IZEs produced shoot and root structures next to embryogenic structures and individual somatic embryos (Figure 7b-e). For this reason, we also scored the shoot/root regeneration efficiency (number of IZEs producing shoots and/or roots; Figure 7a). In the wild type, the SE efficiency reached 94%, 11% of the IZEs produced shoot/roots, and on average 0.73 somatic embryos were produced per IZE. In the *aux1 lax1* double mutant both SE efficiency and SE productivity were significantly decreased (respectively 74% and 0.29) and interestingly, the shoot/root regeneration was significantly increased (51%). For the *aux1 lax2* and *aux1 lax3* double mutants the SE efficiency was not significantly reduced, but the SE productivity was, and these IZEs produced significantly more shoot and roots, (Figure 7a). These findings show that the AUX1/LAX influx proteins act redundantly during SE and are required for SE initiation.

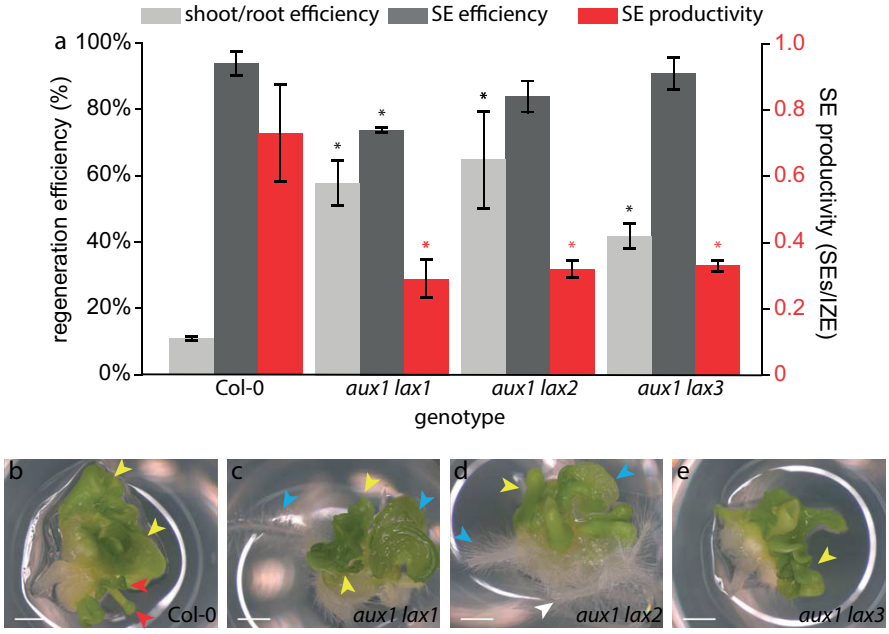

FIGURE 7 - Reduced SE and enhanced shoot/root regeneration in aux1 *lax* loss-of-function mutants.
a) Regeneration efficiencies in wild-type (Col-0), *aux1* lax1, *aux1 lax2,* and *aux1 lax3* IZEs. Bars represent shoot and root efficiency (light gray), SE efficiency (dark grey), and SE productivity (solid red) values of duplo experiments with n = 48. Error bars indicate the SEM. Asterisks denote statistical difference between wild-type control and mutant. For SE efficiency and productivity respectively a $\chi 2$ test and a Welch t-test were used ($p<0.05$) b-e). Phenotypes of b) Col-0 c) *aux1 lax1* d) *aux1 lax2* e) *aux1 lax3* IZEs after standard culture. Red arrow heads point at individual somatic embryos, yellow arrow heads point at embryogenic structures and blue arrow heads indicate shoot- or root-like structures. Scale bar represents 1mm.

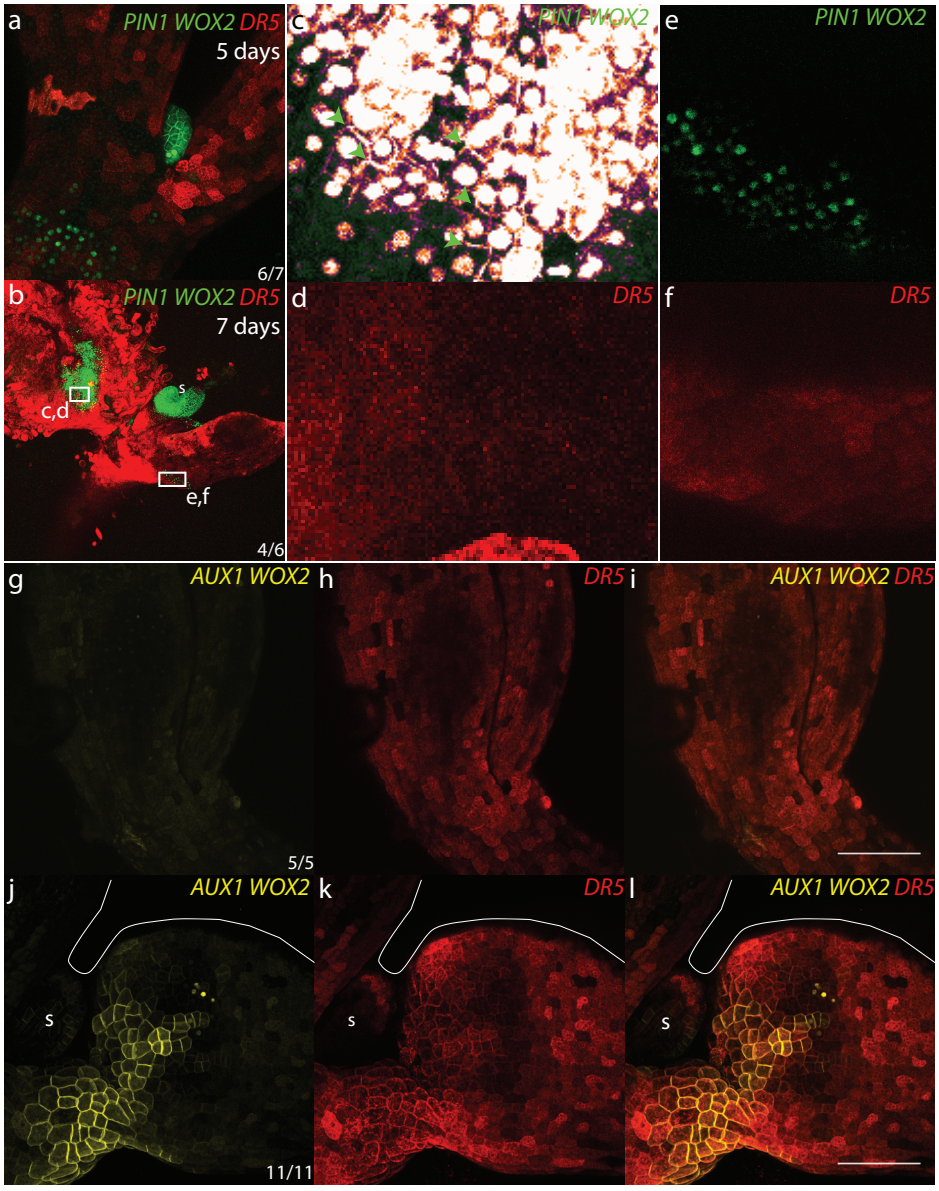

FIGURE 8 - Expression and localisation of PIN1 and AUX1 during 2,4-D induced SE initiation.
a-f) Representative CLSM images of *pPIN1::PIN1:GFP pWOX2::NLS-YFP DR5::RFP* IZEs cultured for a) 5 days and b) 7 days on SEIM. c-f) Enlargements of the boxed regions in (b) with c) a false coloured image of *PIN1* (localised on the membrane, green arrows) and *WOX2* (nuclear localisation) for enhanced contrast and d) *DR5*. e-f) is box 2 with e) *PIN1 WOX2* and f) *DR5*. *PIN1* and *WOX2* are in green, *DR5* in red. g-l) IZEs of *pAUX1::AUX1:YFP pWOX2::NLS-YFP DR5::RFP* cultured on SEIM for g-i) 3 days and j-l) 5 days. *AUX1* and *WOX2* in yellow and *DR5* in red. The shoot apical meristem is marked with an S, observation frequencies are indicated the bottom right corner, scale bar represents 100µm.

Auxin influx is needed to generate auxin response minimum for SE initiation

The previous results suggested that auxin efflux does not contribute to initiation of SE, but rather to the development of the somatic embryo similar to zygotic embryogenesis by establishing the embryo body pattern. To test this hypothesis we studied somatic embryo initiation events in the proximal region of cotyledons of *pPIN1::PIN1-GFP pWOX2::NLS-YFP DR5:RFP* IZEs after 5 and 7 days of culture on SEIM. On day 5, *PIN1::PIN1-GFP* expression was mostly observed in the SAM of the IZE and not in the *WOX2::NLS-YFP* expressing regions where somatic embryos were initiated (Figure 8a). On day 7, however, clusters of *PIN1::PIN1-GFP WOX2::NLS-YFP* positive cells could be observed, and *DR5::RFP* expression in these cell clusters was always low (Figure 8b,c,d). In some areas of low *DR5::RFP* expression we observed cell clusters showing weaker *WOX2::NLS-YFP* and no *PIN1::PIN1-GFP* expression (Figure 8e,f), similar to the *WOX2::NLS-YFP* clusters observed at day5 (Figure 8a). These results are in line with the NPA studies, and indicate that areas of low auxin response that seem to coincide with initiation of SE occur independent of *PIN1* expression, and that *PIN1* only becomes expressed at a later time point after SE initiation, where it is required for embryo patterning. In IZEs that combined the *pAUX1::AUX1:YFP* construct (Swarup et al., 2005) with the *WOX2::NLS-YFP* and *DR5::RFP* reporters no expression of *pAUX1::AUX1:YFP* nor *pWOX2::NLS-YFP* could be detected after 3 days on SEIM (Figure 8g-i). However, after 5 days on SEIM patches of *pAUX1::AUX1:YFP* expressing cells could be observed close to *pWOX2::NLS-YFP* marked cells (Figure 8j-l). The cells expressing *pWOX2::NLS-YFP* were present in low auxin zones, whereas the *pAUX1::AUX1:YFP* expressing cells were part of a zone with a relatively higher auxin response (Figure 8j-l). This finding supports our hypothesis that AUX1/LAX carriers cause local auxin minima in the cotyledons of the IZE resulting into initiation of SE marked by the expression of the *WOX2-YFP* reporter.

Discussion

Somatic embryogenesis is an important tissue culture tool that is used for the stable asexual propagation of economically important crops and ornamentals, and for studying the embryo initiation process for plant species with a long reproductive cycle. For many plant species SE can be induced by treatment of plant tissues with the synthetic auxin analog 2,4-D. Detailed knowledge on the molecular mechanism by which 2,4-D induces SE is lacking, and to gain more insight we optimized the *Arabidopsis* SE system that uses IZEs as explants (Gaj, 2011; Nowak et al., 2012), and studied the role of auxin transport in SE initiation.

A narrow time window for SE induction

Our results showed that the highest and most reproducible SE efficiencies could be obtained using IZEs synchronized in development by manual pollination, and preferably harvested at 12 dap. Opposed to what previous papers report (Luo and Koop, 1997; Gaj, 2004), we experienced that IZEs harvested at earlier time points do not survive when cultured on SEIM. Apparently, sufficient maturation of the IZE is important for its survival in tissue culture. Several lines of evidence back up this idea as the embryogenic capacity of tissues is enhanced by dehydration and osmotic stresses (Ikeda-Iwai et al., 2003; Gazzarrini et al., 2004). The well-known spontaneous SE phenotypes of seedlings ectopically expressing *LEC1*, *LEC2* or *FUS3* also support the idea that tissue maturation is a central mechanism in SE. These *LAFL* genes have initially been identified because of their role in seed maturation and their dependency on seed maturation hormone ABA. By ectopically expressing *LEC1*, *LEC2* and *FUS3*, the seedling development is arrested and most likely reverted to the embryo maturation phase, resulting in prolonged embryo identity and SE initiation (Stone et al., 2008; Junker et al., 2012; Su et al., 2012; Jia et al., 2013). In contrast to these systems, in our 2,4-D SE inducible system, in which SE efficiency is dependent on the age of the IZE, it is necessary to take other factors into account. One of them is, the maternal environment in which seeds develop, as it determines the vigour of the IZEs (Finch-Savage and Bassel, 2016). For reproducible SE efficiencies the growth conditions should therefore be kept constant.

With our optimised culture system we were able to show, using the *pWOX2::NLS-YFP* reporter as embryonic cell marker (Breuninger et al., 2008), that the first reversions from somatic to embryonic cell identity occurred between 5 and 7 days in culture. Our results showed that the development of the somatic embryo could be traced from single cells to globular shaped embryos and the earliest embryonic cell clusters could be observed after 5 days of 2,4-D induction. However, transfer to hormone free medium at this time point resulted in loss of *WOX2* expression and reverted the tissue to the germination programme. Thus there is a narrow time frame in which IZEs can be used as explants for SE efficiently, between 12 and 14 dap, and a minimum time of 5 days on SEIM is required to induce SE. Our system allows for studying real-time dynamic molecular responses as opposed to classic histology studies, which have relied on destructive methods (Raghavan, 2004; Bassuner et al., 2006; Kurczyńska et al., 2007; Soriano et al., 2013). Other reports have shown the use of the *WUSCHEL (WUS)* shoot apical meristem (SAM) stem cell fate reporter, as a marker for SE (Su and Zhang, 2009), but this reporter would only show cells that have already adapted the stem cell

fate (Mayer et al., 1998; Strable and Scanlon, 2016) and is therefore not accurate to identify the transition from late to early embryogenic cell fate.

An auxin minimum is compulsory for SE initiation

Previous reports have indicated that, similar to ZE, dynamic auxin responses starting with an auxin maximum are the main drivers of SE (Michalczuk et al., 1992; Pasternak, 2002; Gaj et al., 2005; Su et al., 2015). In line with these reports, by combining the *pWOX2::NLS-YFP* marker with the *DR5::RFP* auxin reporter, we were able to show that after 5 days of culture the overall auxin response in IZEs was elevated. Surprisingly, however, local auxin minima were established in which cells acquired embryo identity. Our results showed that PINs were not required for SE initiation and that the observed local auxin response minima were not produced by coordinated PIN mediated auxin efflux. This is contradictory to a previous hypothesis in which it was proposed that PIN1 mediates auxin from high to low areas in order to induce SE (Su et al., 2009). It is also in contrast to the auxin maximum marking the early embryo proper during ZE, and to the PIN generated auxin maxima that are initiation points for lateral organ development such as leaves and flowers on the shoot- or inflorescence meristems, and lateral roots on the root pericycle (Benková et al., 2003; Reinhardt et al., 2003). Treatment of IZEs with the polar auxin transport inhibitor NPA did result in aberrant, fused embryonic structures, indicating that, similar to ZE, PIN driven PAT is rather involved in development and patterning of the somatic embryo (Friml et al., 2003; Robert et al., 2013).

Interestingly, in contrast to auxin efflux, the AUX1/LAX auxin influx proteins appeared to be required for SE initiation. The role of AUX1/LAX is well established during root growth and development (Bennett et al., 1996;; Peret et al., 2012), in phyllotaxis (Reinhardt 2003; Bainbridge et al., 2008), and also in ZE (Robert et al., 2015b). However, except for recent evidence that *LAX3* is expressed during SE (Revalska et al., 2015), no role for the AUX1/LAX proteins during SE has yet been reported The proposed function of the AUX/LAX proteins is to keep auxin contained in cells, and recent auxin transport measurements confirmed an important role for AUX1/LAX proteins in loading auxin into the PAT system (Boot et al., 2016). Similarly, we hypothesize that the coordinated expression of AUX/LAX proteins keeps endogenous auxin contained in specific cells of the IZE, thereby enhancing auxin response in these cells and simultaneously causing an auxin response minimum in other regions of the IZE. In the absence of auxin minima in 1-NOA and 2,4-D treated IZEs, the balance shifted from SE to organ regeneration, which confirms the importance of auxin minima for the induction of embryonic cell identity, and is in line with the requirement of auxin maxima

for organ initiation (Benkova, et al., 2003, Reinhardt et al., 2003). We cannot point out AUX1/LAX-mediated auxin influx as the sole responsible mechanism for SE initiation. Evidence is emerging that oscillating auxin responses resulting from dynamic changes in auxin signalling, -biosynthesis or -metabolism contribute to organ initiation, meristem establishment and embryo patterning (Xuan et al., 2015; Wang et al., 2014; Robert et al., 2013).

Methods

Plant lines

All *Arabidopsis thaliana* lines described below are in Columbia (Col-0) background. The *pWOX2::NLS-YFP* line was kindly donated by Thomas Laux and is resistant to phosphinothricin (ppt) (Breuninger et al., 2008). The *DR5::RFP* line was donated by Eva Benkova and is resistant to hygromycin (hyg) (Marhavý et al., 2011). *AUX1::AUX1-YFP* harbours kanamycin (kan) resistance and was donated by Malcom Bennet (Swarup et al., 2005). *PIN1::PIN1-GFP* (kan) was a gift from Jiri Friml (Benková et al., 2003). The *aux1 lax* double mutants were a gift from Ranjan Swarup (Peret et al., 2012). The *aux1* mutation was verified by growing seedlings on 0.1µM 2,4-D and seedlings were selected based on their resistance to 2,4-D. The other mutations were confirmed by genotyping.

Genotyping

Sequences of DNA primers used for genotyping of the *aux lax* double mutants are in listed in Table S1. All PCR reactions were performed using DreamTaq DNA polymerase (ThermoFisher Scientific, EP0705) on genomic DNA isolated as described by Giraudat (2003), Tm = 61°C, and At = 60s, unless otherwise stated.

Tissue culture and growth conditions

Arabidopsis seeds were surface sterilized and germinated on MA medium (Masson and Paszkowski, 1992) complemented with 1% (w:v) sucrose, and 0.8% (w:v) Daishin agar, pH5.8. For antibiotic selection ppt, hyg or kan was added to the medium after autoclaving at a final concentration of 20mg/mL for ppt and hyg, and of 50mg/mL for kan. Seven to ten days after germination (dag), seedlings were transferred to a mixture of soil and sand, 2 per pot, and grown under a 16hr. photoperiod and 70% relative humidity. IZEs were harvested from plants 1-2 weeks after flowering. The siliques were surface sterilized with a 20% bleach/70% ethanol solution for 5min. and rinsed at least three times with sterile water.

SE-inducing medium (SEIM) consisted of B5 medium, with 4.5µM 2,4-D, 2% (w:v) sucrose and 0.8% (w:v) Daishin agar (Gaj, 2011; Nowak et al., 2012). Hormone free medium was MA medium (Masson and Paszkowski, 1992). Media were sterilized by autoclaving at 120°C for 20min. SE was performed in sterile 48-wells plates (Greiner cellstar art. nr. 677180) that were filled with 400µL SEIM or hormone free medium using a repeater pipet. IZEs were placed on SEIM (one per well) and incubated overnight at 4°C in the dark followed by incubation at 21°C under a 16hr photoperiod for a standard period of 14 days, followed by 7 days incubation on hormone free medium (standard SE culture). NPA (CAS 132-66-1) and 1-NOA (CAS 2976-75-1) were ordered from Sigma and were added to SEIM from a 50mM stock solution in DMSO to a final concentration of 100µM.

For the inhibitor and phenotypic studies, IZEs synchronized in their developmental stage were obtained by manual pollination. For this purpose, the 2 or 3 oldest, but still closed, flower buds of primary inflorescence stems were emasculated and pollinated and 12 days after pollination (dap) IZEs were excised from the ovule using a dissecting microscope. Per two parent plants, 2-3 sets of 2-3 closed flower buds were emasculated.

To keep data comparable between inhibitor experiments, large-scale experiments were set up as follows: each replicate consisted of 100µM NPA, 100µM 1-NOA and control treatments with 2,4-D induction periods for 0, 3 and 5 days. Per treatment, 48 IZEs were used, one IZE per well in a 48-wells plate. For the 3 and 5 days induction, a large pool of IZEs was cultured in multiple 48-wells plates. At day 3 and day 5 48 IZEs were selected randomly out of the different plates for each treatment and transferred to plates containing 2,4-D and 100µM inhibitor. The day 0 treatments were set up differently: 1 silique was used to take 12 IZEs for each treatment; this required 4 siliques in total to compile 1 plate per treatment.

The mutant studies were performed by culturing 48 IZEs per genotype in duplicates.

For confocal or light microscopy analysis non-synchronized late IZEs from more or less the same developmental stage were selected based on their size as described by (Gaj, 2011). Broken or damaged IZEs were discarded and not used.

Statistics of somatic embyogenesis

To quantify SE, four categories were used to score 1) embryogenic tissue (also referred to as embryogenic callus), if no individual somatic embryos were found but embryogenic tissue developed. Embryogenic tissue was defined as smooth green structures without trichomes, that either looked like fused cotyledons or like fused zygotic embryos 2) SE forming IZEs, if individual somatic embryos

were observed that were attached to the IZE by their root pole. In that case, the number of individual somatic embryos was counted. 3) Non-embryogenic callus forming IZEs, if callus was formed that remained white-yellowish without developing somatic embryos or embryogenic tissue 4) Dead IZEs that turned white, if the tissue turned white, showed no growth and maintained their original size.

Category 1 and 2 were merged to quantify the number of responding IZEs that produced embryogenic tissue. The SE efficiency was then calculated as (Luo and Koop, 1997)

$$SE\ efficiency = \frac{N_r}{N_t} \quad 100\%$$

N_r = the number of responding explants. N_t = total number of explants tested.

SE productivity was calculated as

$$SE\ productivity = \frac{N_i}{N_t}$$

N_i = the number of individual somatic embryos observed. N_t = the total number of IZEs that were tested (including the ones that died).

Statistics for SE efficiency were performed in Microsoft Excel, using the χ^2-test for association (Holmes et al., 2011). For SE productivity, a Welch *t*-test was performed in Rstudio (Pace, 2015).
For inhibitor studies we compared the control treatments to check whether refreshment of SEIM would contribute to SE efficiency and productivity. The two controls were not statistically different for SE efficiency and productivity (respectively χ^2_{calc}=2.9, and *t*-test p-value 0.524, described in Chapter 2) and for this reason we performed all statistical tests between the treatment and the 0 days control.

Microscopy

Confocal Laser Scanning Microscopy (CLSM) was performed with a ZEISS LSM510 exciter equipped with argon and helium/neon lasers. GFP and YFP were detected using a 488nm band pass filter for excitation and a 500-530nm band pass (BP) filter for emission. Simultaneously, chlorophyll background fluorescence was captured with a long pass (LP) 650nm emission filter. RFP was excited at 530nm and was captured with a BP 550-600nm emission filter. Images were captured with ZEISS ZEN2009 software. Samples were prepared on a microscope slide by

embedding IZEs in a thin layer of 0.5% low melting point agarose, and adding a droplet of water before covering with a cover slip.
Phenotype images were obtained using a Leica DC 500 stereomicroscope with the Leica Application Suite v2.8.1 software or with a MRc5 (ZEISS) microscope with DIC/Nomarski ZEISS AxioCam using AxioVision40 V4.7.2.0 software.

Acknowledgements

C.P. was supported by an NWO-TTI-Green Genetics core project grant (NWO 828.11.004) to R.O. from the Earth and Life Sciences Division with financial support from the Netherlands Organisation for Scientific Research (NWO). We thank Gerda Lamers for her help with microscopy.

Supplemental Information

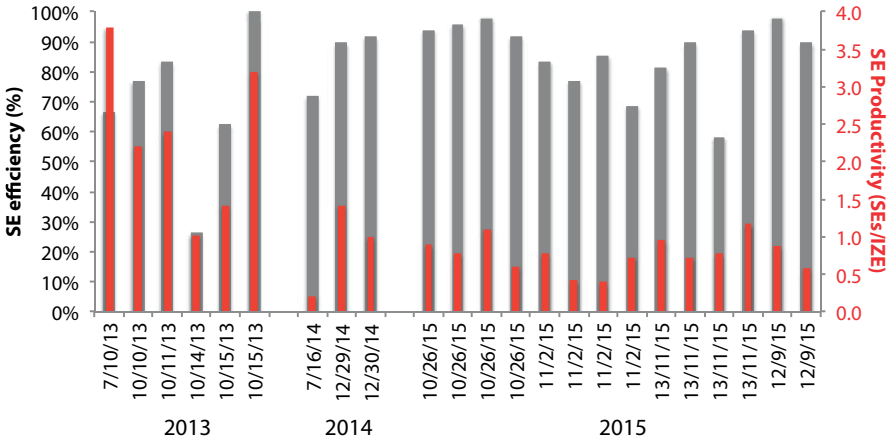

FIGURE S1 - Variation in SE efficiency and SE productivity. Per experiment SE efficiency (grey bars and left axis) and SE productivity (red bars and right axis) are indicated. Values are given for experiments in the course of 2013, 2014 and 2015.

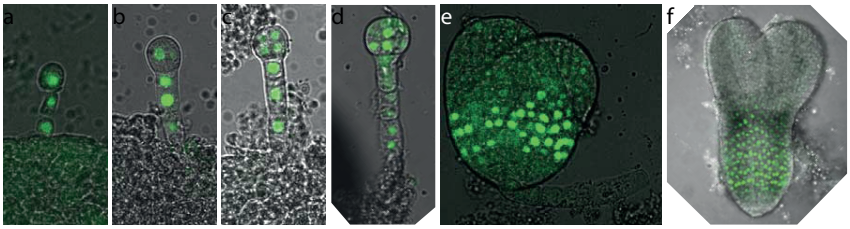

FIGURE S2 - Expression pattern of the embryo cell fate marker WOX2-YFP in Arabidopis. Representative CSLM images of pWOX2::NLS-YFP (green) in the 1-cellstage (a), 2-cell stage (b), octant- cell stage (c), early globular stage (d), late heart stage (e), torpedo stage (f). WOX2-YFP was observed from the zygotic stage onwards, in the entire embryo and suspensor. In later stages, expression diminishes and becomes limited to the hypocotyl area.

TABLE S1 - Primer sequences for genotyping. GSP is gene specific primer, BP is border specific primer. All reactions were carried out with genomic DNA, DreamTaq polymerase, Tm = 61°C, At = 60s, unless otherwise stated.

GENE	PRIMER ORIENTATION	SEQUENCE (5' - 3')	REMARKS
lax1	GSP left	ATATGGTTGCAGGTGGCACA	
	GSP right	GTAACCGGCAAAAGCTGCA	
	Border	AAGCACGACGGCTGTAGAATAG	in combination with GSP left primer for transposon insertion
lax2	GSP left	ATGGAGAACGGTGAGAAAGCAGC	
	GSP right	CGCAGAAGGCAGCGTTAGCG	
	Border	AAGCACGACGGCTGTAGAATAG	in combination with GSP left primer for transposon insertion
lax3	GSP left	TACTTCACCGGAGCCACCA	
	GSP right	TGATTGGTCC GAAAAAGG	
	Border	AAGCACGACGGCTGTAGAATAG	in combination with GSP left primer for transposon insertion

References

Arnold, S. von, Sabala, I., Bozhkov, P., Dyachok, J., and Filonova, L. (2002). Developmental pathways of somatic embryogenesis. Plant Cell. Tissue Organ Cult. **69**: 233–249.

Bainbridge, K., Guyomarc'h, S., Bayer, E., Swarup, R., Bennett, M., Mandel, T., and Kuhlemeier, C. (2008). Auxin influx carriers stabilize phyllotactic patterning. Genes Dev. **22**: 810–823.

Bairu, M.W., Aremu, A.O., and van Staden, J. (2011). Somaclonal variation in plants: causes and detection methods. Plant Growth Regul. **63**: 147–173.

Bassuner, B.M., Lam, R., Lukowitz, W., and Yeung, E.C. (2006). Auxin and root initiation in somatic embryos of *Arabidopsis*. Plant Cell Rep. **26**: 1–11.

Benková, E., Michniewicz, M., Sauer, M., Teichmann, T., Seifertová, D., Jürgens, G., and Friml, J. (2003). Local, efflux-dependent auxin gradients as a common module for plant organ formation. Cell **115**: 591–602.

Blilou, I., Xu, J., Wildwater, M., Willemsen, V., Paponov, I., Friml, J., Heidstra, R., Aida, M., Palme, K., and Scheres, B. (2005). The PIN auxin efflux facilitator network controls growth and patterning in *Arabidopsis* roots. Nature **433**: 39–44.

Boot, K.J.M., Hille, S.C., Libbenga, K.R., Peletier, L.A., van Spronsen, P.C., van Duijn, B., and Offringa, R. (2015). Modelling the dynamics of polar auxin transport in inflorescence stems of *Arabidopsis* thaliana. J. Exp. Bot. **67:** 649-666.

Boutilier, K., Offringa, R., Sharma, V.K., Kieft, H., Ouellet, T., Zhang, L., Hattori, J., Liu, C., van Lammeren, A.A.M., Miki, B.L.A., Custers, J.B.M., and van Lookeren Campagne, M.M. (2002). Ectopic expression of *BABY BOOM* triggers a conversion from vegetative to embryonic growth. Plant Cell **14**: 1737–1749.

Breuninger, H., Rikirsch, E., Hermann, M., Ueda, M., and Laux, T. (2008). Differential expression of WOX Genes mediates apical-basal axis formation in the *Arabidopsis* embryo. Dev. Cell **14**: 867–876.

Cheng, Y. (2006). Auxin biosynthesis by the YUCCA flavin monooxygenases controls the formation of floral organs and vascular tissues in *Arabidopsis*. Genes Dev. **20**: 1790–1799.

FAO (2015). 2014 Global forest products facts and figures. Food Agric. Organ. United Nations: 1–17.

Fehér, A. (2015). Somatic embryogenesis — Stress-induced remodeling of plant cell fate. Biochim. Biophys. Acta - Gene Regul. Mech. **1849**: 385–402.

Finch-Savage, W.E. and Bassel, G.W. (2016). Seed vigour and crop establishment: extending performance beyond adaptation. J. Exp. Bot. **67**: 567–591.

Friml, J., Benková, E., Blilou, I., Wisniewska, J., Hamann, T., Ljung, K., Woody, S., Sandberg, G., Scheres, B., and Jürgens, G. (2002). AtPIN4 mediates sink-driven auxin gradients and root patterning in *Arabidopsis*. Cell **108**: 661–673.

Friml, J., Vieten, A., Sauer, M., Weijers, D., Schwarz, H., Hamann, T., Offringa, R., and Jürgens, G. (2003). Efflux-dependent auxin gradients establish the apical-basal axis of *Arabidopsis*. Nature **426**: 147–153.

Gaj, M.D. (2001). Direct somatic embryogenesis as a rapid and efficient system for in vitro regeneration of *Arabidopsis* thaliana. Plant Cell. Tissue Organ Cult. **64**: 39–46.

Gaj, M.D. (2004). Factors influencing somatic embryogenesis induction and plant regeneration with particular reference to *Arabidopsis* thaliana (L.) Heynh. Plant Growth Regul. **43**: 27–47.

Gaj, M.D. (2011). Somatic embryogenesis and plant regeneration in the culture of *Arabidopsis thaliana* (L.) Heynh. immature zygotic embryos. Methods **710**: 257–265.

Gaj, M.D., Zhang, S., Harada, J.J., and Lemaux, P.G. (2005). Leafy cotyledon genes are essential for induction of somatic embryogenesis of *Arabidopsis*. Planta **222**: 977–988.

Ganguly, A., Park, M., Kesawat, M.S., and Cho, H.-T. (2014). Functional analysis of the hydrophilic loop in intracellular trafficking of *Arabidopsis* PIN-FORMED proteins. Plant Cell **26**: 1570–1585.

Gazzarrini, S., Tsuchiya, Y., Lumba, S., Okamoto, M., and McCourt, P. (2004). The transcription factor *FUSCA3* controls developmental timing in *Arabidopsis* through the hormones gibberellin and abscisic acid. Dev. Cell **7**: 373–385.

Geisler, M. and Murphy, A.S. (2006). The ABC of auxin transport: The role of p-glycoproteins in plant development. FEBS Lett. **580**: 1094–1102.

Giraudat, J. (2003). Practical course on genetic and molecular analysis of *Arabidopsis*. In EMBO course, J. Giraudat, ed (EMBO), pp. 1–21.

Goldsmith, M.H.M. (1977). The polar transport of auxin. Annu. Rev. Plant Physiol. **28**: 439–478.

Haecker, A., Gross-Hardt, R., Geiges, B., Sarkar, A., Breuninger, H., Herrmann, M., and Laux, T. (2004). Expression dynamics of *WOX* genes mark cell fate decisions during early embryonic patterning in *Arabidopsis thaliana*. Development **131**: 657–668.

Hardtke, C.S. and Berleth, T. (1998). The *Arabidopsis* gene *MONOPTEROS* encodes a transcription factor mediating embryo axis formation and vascular development. EMBO J. **17**: 1405–1411.

Heisler, M.G., Ohno, C., Das, P., Sieber, P., Reddy, G. V, Long, J. A, and Meyerowitz, E.M. (2005). Patterns of auxin transport and gene expression during primordium development revealed by live imaging of the *Arabidopsis* inflorescence meristem. Curr. Biol. **15**: 1899–1911.

Holmes, D., Moody, P., and Dine, D. (2011). Research methods for biosciences 2nd ed. O. university Press, ed (Oxford University Press).

Ikeda-Iwai, M., Umehara, M., Satoh, S., and Kamada, H. (2003). Stress-induced somatic embryogenesis in vegetative tissues of *Arabidopsis thaliana*. Plant J. **34**: 107–114.

Jia, H., McCarty, D.R., and Suzuki, M. (2013). Distinct roles of *LAFL* network genes in promoting the embryonic seedling fate in the absence of *VAL* repression. Plant Physiol. **163**: 1293–1305.

Jiménez, V.M. (2005). Involvement of plant hormones and plant growth regulators on in vitro somatic embryogenesis. Plant Growth Regul. **47**: 91–110.

Jones, A.R., Kramer, E.M., Knox, K., Swarup, R., Bennett, M.J., Lazarus, C.M., Leyser, H.M.O., and Grierson, C.S. (2009). Auxin transport through non-hair cells sustains root-hair development. Nat. Cell Biol. **11**: 78–84.

Junker, A. Mönke, G., Rutten, T., Keilwagen, J., Seifert., Thi, T.M.N., Renou, J., Balzergue, S., Viehöver, P., Hähnel, U., Ludwig-Müller, J., Altschmied, L., Conrad, U., Weisshaar, B., and Bäumlein, H. (2012). Elongation-related functions of *LEAFY COTYLEDON1* during the development of *Arabidopsis thaliana*. Plant J. **71**: 427–442.

Kurczyńska, E.U., Gaj, M.D., Ujczak, A., and Mazur, E. (2007). Histological analysis of direct somatic embryogenesis in *Arabidopsis thaliana* (L.) Heynh. Planta **226**: 619–628.

Lotan, T., Ohto, M., Yee, K.M., West, M. A, Lo, R., Kwong, R.W., Yamagishi, K., Fischer, R.L., Goldberg, R.B., and Harada, J.J. (1998). *Arabidopsis LEAFY COTYLEDON1* is sufficient to induce embryo development in vegetative cells. Cell **93**: 1195–1205.

Luo, Y. and Koop, H.U. (1997). Somatic embryogenesis in cultured immature zygotic embryos and leaf protoplasts of *Arabidopsis thaliana* ecotypes. Planta **202**: 387–96.

Luschnig, C., Gaxiola, R.A., Grisafi, P., and Fink, G.R. (1998). EIR1, a root specific protein involved in auxin transport, is required for gravitropism in *Arabidopsis* thaliana. Genes Dev. **12**: 2175–2187.

Marchant, A., Bhalerao, R., Casimiro, I., Eklöf, J., Casero, P.J., Bennett, M., and Sandberg, G. (2002). AUX1 promotes lateral root formation by facilitating indole-3-acetic acid distribution between sink and source tissues in the *Arabidopsis* seedling. Plant Cell **14**: 589–97.

Marhavý, P., Bielach, A., Abas, L., Abuzeineh, A., Duclercq, J., Tanaka, H., Pařezová, M., Petrášek, J., Friml, J., Kleine-Vehn, J., and Benková, E. (2011). Cytokinin modulates endocytic trafficking of PIN1 auxin efflux carrier to control plant organogenesis. Dev. Cell **21**: 796–804.

Marhavý, P., Vanstraelen, M., De Rybel, B., Zhaojun, D., Bennett, M.J., Beeckman, T., and Benková, E. (2013). Auxin reflux between the endodermis and pericycle promotes lateral root initiation. EMBO J. **32**: 149–158.

Mayer, K.F.X., Schoof, H., Haecker, A., Lenhard, M., Jürgens, G., and Laux, T. (1998). Role of *WUSCHEL* in regulating stem cell fate in the *Arabidopsis* shoot meristem. Cell **95**: 805–815.

Michalczuk, L., Ribnicky, D.M., Cooke, T.J., and Cohen, J.D. (1992). Regulation of indole-3-acetic acid biosynthetic pathways in carrot cell cultures. Plant Physiol. **100**: 1346–1353.

Mravec, J., Petr Skupa, Bailly, A., Hoyerova, K., Křeček, Bielach, A., Petrášek, J., Zhang, J., Gaykova, V., Stierhof, Y-D., Dobrev P.I., Schwarzerova, K., Rolčík, J., Seifertová, D., Luschnig, C., Benková, E., Zažímalova, E., Geisler, M., Friml, J. (2009). Subcellular homeostasis of phytohormone auxin is mediated by the ER-localized PIN5 transporter. Nature **459**: 1136–1140.

Mravec, J., Kubes, M., Bielach, A., Gaykova, V., Petrásek, J., Skůpa, P., Chand, S., Benková, E., Zazímalová, E., and Friml, J. (2008). Interaction of PIN and PGP transport mechanisms in auxin distribution-dependent development. Development **135**: 3345–3354.

Noh, B., Murphy, A.S., and Spalding, E.P. (2001). Multidrug resistance-like genes of *Arabidopsis* required for auxin transport and auxin-mediated development. Plant Cell **13**: 2441–2454.

Nowak, K., Wojcikowska, B., Szyrajew, K., and Gaj, M.D. (2012). Evaluation of different embryogenic systems for production of true somatic embryos in *Arabidopsis*. Biol. Plant. **56**: 401–408.

Pace, L. (2015). Beginning R: an introduction to statistical programming (Apress).

Parry, G., Delbarre, A., Marchant, A., Swarup, R., Napier, R., Perrot-Rechenmann, C., and Bennett, M.J. (2001). Novel auxin transport inhibitors phenocopy the auxin influx carrier mutation aux1. Plant J. **25**: 399–406.

Pasternak, T.P. (2002). The role of auxin, pH, and stress in the activation of embryogenic cell division in leaf protoplast-derived cells of Alfalfa. Plant Physiol. **129**: 1807–1819.

Péret, B., Swarup, K., Ferguson, A., Seth, M., Yang, Y., Dhondt, S., James, N., Casimiro, I., Perry, P., Syed, A., Yang, H., Reemmer, J., Venison, E., Howells, C., Perez-Amador, M-A., Yun, J., Alonso, J., Beemster, G.T.S., Laplaze, L., Murphy, A., Bennett, M.J., Nielsen, E., and Swarup, R. (2012). AUX/LAX genes encode a family of auxin influx transporters that perform distinct functions during *Arabidopsis* development. Plant Cell **24**: 2874–2885.

Petrášek, J., Mravec, J., Bouchard, R., Blakeslee, J.J., Abas, M., Seifertová , D., Wiśniewska, J., Tadele, Z., Kubeš, M., Cővanová., M., Dhonukshe, P., Skupa, P., Benková, E., Perry, L., Křeček, P., Lee, O.K.., Fink, G.R., Geisler, M., Murphy, A.S., Luschnig, L., Zažímalova, E., and Friml, J. (2006). PIN proteins perform a rate-limiting function in cellular auxin efflux. Science **312**: 914–918.

Petrásek, J. and Friml, J. (2009). Auxin transport routes in plant development. Development **136**: 2675–88.

Pupilli, F. and Barcaccia, G. (2012). Cloning plants by seeds: inheritance models and candidate genes to increase fundamental knowledge for engineering apomixis in sexual crops. J. Biotechnol. **159**: 291–311.

Rademacher, E.H., Lokerse, A.S., Schlereth, A., Llavata-Peris, C., Bayer, M., Kients, M., Rios, A.F., Borst, J.W., Lukowitz, W., Jürgens, G., and Weijers, D. (2012). Different auxin response machineries control distinct cell fates in the early plant embryo. Dev. Cell **22**: 211–222.

Raghavan, V. (2004). Role of 2,4-dichlorophenoxyacetic acid (2,4-D) in somatic embryogenesis on cultured zygotic embryos of *Arabidopsis*: cell expansion, cell cycling, and morphogenesis during continuous exposure of embryos to 2,4-D. Am. J. Bot. **91**: 1743–1756.

Raven, J.A. (1975). Transport of indoleacetic acid in plant cells in relation to pH and electrical potential gradients, and its significance for polar IAA transport. New Phytol.: 163–172.

Reinhardt, D., Mandel, T., and Kuhlemeier, C. (2000). Auxin regulates the initiation and radial position of plant lateral organs. Plant Cell **12**: 507–518.

Reinhardt, D., Pesce, E.-R., Stieger, P., Mandel, T., Baltensperger, K., Bennett, M., Traas, J., Friml, J., and Kuhlemeier, C. (2003). Regulation of phyllotaxis by polar auxin transport. Nature **426**: 255–260.

Revalska, M., Vassileva, V., Zechirov, G., and Iantcheva, A. (2015). Is the auxin influx carrier *LAX3* essential for plant growth and development in the model plants *Medicago truncatula*, *Lotus japonicus* and *Arabidopsis thaliana* Biotechnol. Biotechnol. Equip. **29**: 786–797.

Robert, H.S., Crhak Khaitova, L., Mroue, S., and Benkova, E. (2015a). The importance of localized auxin production for morphogenesis of reproductive organs and embryos in *Arabidopsis*. J. Exp. Bot. **66**: 5029–5042.

Robert, H.S., Grunewald, W., Sauer, M., Cannoot, B., Soriano, M., Swarup, R., Weijers, D., Bennett, M., Boutilier, K., and Friml, J. (2015b). Plant embryogenesis requires AUX/LAX-mediated auxin influx. Development **142**: 702–711.

Robert, H.S., Grones, P., Stepanova, A.N., Robles, L.M., Lokerse, A.S., Alonso, J.M., Weijers, D., and Friml, J. (2013). Local auxin sources orient the apical-basal axis in *Arabidopsis* embryos. Curr. Biol. **23**: 2506–2512.

Rubery, P.H. and Sheldrake, A.R. (1974). Carrier-mediated auxin transport. Planta **118**: 101–121.

Sawchuk, M.G., Edgar, A., and Scarpella, E. (2013). Patterning of leaf vein networks by convergent auxin transport pathways. PLoS Genet. **9**: e1003294.

De Smet, I., Tetsumura, T., De Rybel, B., Frei dit Frey, N., Laplaze, L., Casimiro, I., Swarup, R., Naudts, M., Vanneste, S., Audenaert, D., Inzé, D., Bennet, M.J., and Beeckman, T. (2007). Auxin-dependent regulation of lateral root positioning in the basal meristem of *Arabidopsis*. Development 134: 681–690.

Soriano, M., Li, H., and Boutilier, K. (2013). Microspore embryogenesis: establishment of embryo identity and pattern in culture. Plant Reprod. **26**: 181–196.

Stone, S.L., Braybrook, S. a, Paula, S.L., Kwong, L.W., Meuser, J., Pelletier, J., Hsieh, T.-F., Fischer, R.L., Goldberg, R.B., and Harada, J.J. (2008). *Arabidopsis LEAFY COTYLEDON2* induces maturation traits and auxin activity: Implications for somatic embryogenesis. Proc. Natl. Acad. Sci. **105**: 3151–3156.

Stone, S.L., Kwong, L.W., Yee, K.M., Pelletier, J., Lepiniec, L., Fischer, R.L., Goldberg, R.B., and Harada, J.J. (2001). *LEAFY COTYLEDON2* encodes a B3 domain transcription factor that induces embryo development. Proc. Natl. Acad. Sci. USA **98**: 11806–11811.

Strable, J. and Scanlon, M.J. (2016). Meristems take their cues from organ primordia. Nat. Genet. **48**: 704–705.

Su, Y.H., Liu, Y.B., Bai, B., and Zhang, X.S. (2015). Establishment of embryonic shoot-root axis is involved in auxin and cytokinin response during *Arabidopsis* somatic embryogenesis. Front. Plant Sci. **5**: 1–9.

Su, Y.H., Su, Y.X., Liu, Y.G., and Zhang, X.S. (2012). Abscisic acid is required for somatic embryo initiation through mediating spatial auxin response in *Arabidopsis*. Plant Growth Regul.

Su, Y.H. and Zhang, X.S. (2009). Auxin gradients trigger de novo formation of stem cells during somatic embryogenesis. Plant Signal. Behav. **4**: 574–576.

Su, Y.H., Zhao, X.Y., Liu, Y.B., Zhang, C.L., O'Neill, S.D., and Zhang, X.S. (2009). Auxin-induced *WUS* expression is essential for embryonic stem cell renewal during somatic embryogenesis in *Arabidopsis*. Plant J. **59**: 448–60.

Swarup, K., Benková, E., Swarup, R., Casimiro, I., Péret, B., Yang, Y., Parry, G., Nielsen, E., De Smet, I., Vanneste, S., Levesque, M.P., Carrier, D., James, N., Calvo, V., Ljung, K., Kramer, E., Roberts, R., Graham, N., Marillonnet, S., Patel, K., Jones, J.D.G., Taylor, G., Schachtman, D.P., May, S., Sandberg, G., Benfey, P., Friml, J., Kerr, I., Beeckman, T., Laplaze, L., and Bennet, M.J. (2008). The auxin influx carrier LAX3 promotes lateral root emergence. Nat. Cell Biol. **10**: 946–954.

Swarup, R., Friml, J., Marchant, A., Ljung, K., Sandberg, G., Palme, K., and Bennett, M. (2001). Localization of the auxin permease AUX1 suggests two functionally distinct hormone transport pathways operate in the *Arabidopsis* root apex. Genes Dev. **15**: 2648–2653.

Swarup, R., Kramer, E.M., Perry, P., Leyser, O., Knox, K., Beemster, G.T.S., Haseloff, J., Bhalerao, R., and Bennett, M.J. (2005). Root gravitropism requires lateral root cap and epidermal cells for transport and response to a mobile auxin signal. Nat. Cell Biol. **7**: 1057–1065.

Swarup, R. and Péret, B. (2012). *AUX/LAX* family of auxin influx carriers—an overview. Front. Plant Sci. **3**: 1–11.

Timmis, R. (1998). Bioprocessing for tree production in the forest industry: conifer somatic embryogenesis. Biotechnol. Prog. **14**: 156–166.

Ugartechea-Chirino, Y., Swarup, R., Swarup, K., Péret, B., Whitworth, M., Bennett, M., and Bougourd, S. (2010). The *AUX1/LAX* family of auxin influx carriers is required for the establishment of embryonic root cell organization in *Arabidopsis thaliana*. Ann. Bot. **105**: 277–289.

Ulmasov, T., Murfett, J., Hagen, G., and Guilfoyle, T.J. (1997). Aux/IAA proteins repress expression of reporter genes containing natural and highly active synthetic auxin response elements. Plant Cell **9**: 1963–71.

Wang, Q., Kohlen, W., Rossmann, S., Vernoux, T., and Theres, K. (2014). Auxin depletion from the leaf axil conditions competence for axillary meristem formation in *Arabidopsis* and *Tomato*. Plant Cell **26**: 2068–2079.

Weijers, D., Sauer, M., Meurette, O., Friml, J., Ljung, K., Sandberg, G., Hooykaas, P., and Offringa, R. (2005). Maintenance of embryonic auxin distribution for apical-basal patterning by PIN-FORMED-dependent auxin transport in *Arabidopsis*. Plant Cell **17**: 2517–2526.

Weijers, D., Schlereth, A., Ehrismann, J.S., Schwank, G., Kientz, M., and Jürgens, G. (2006). Auxin triggers transient local signaling for cell specification in *Arabidopsis* embryogenesis. Dev. Cell **10**: 265–270.

Wisniewska, J. (2006). Polar PIN localization directs auxin flow in plants. Science (80-.). **312**: 883–883.

Xuan, W., Audenaert, D., Parizot, B., Möller, B.K., Njo, M.F., De Rybel, B., De Rop, G., Van Isterdael, G., Mähönen, A.P., Vanneste, S., and Beeckman, T. (2015). Root cap-derived auxin pre-patterns the longitudinal axis of the *Arabidopsis* root. Curr. Biol. **25**: 1381–1388.

Zuo, J., Niu, Wu, Q.-W., Frugis, G., and Chua, N-H. (2002). The *WUSCHEL* gene promotes vegetative-to-embryonic transition in *Arabidopsis*. Plant J. **30**: 349–359.